Atmospheric Environment 45 (2011) 7143–7150

Contents lists available at ScienceDirect

Atmospheric Environment

journal homepage: www.elsevier.com/locate/atmosenv

Ozone air quality measurement requirements for a geostationary satellite mission

Peter Zoogman [a,*], Daniel J. Jacob [a,b], Kelly Chance [c], Lin Zhang [a], Philippe Le Sager [b,1], Arlene M. Fiore [d], Annmarie Eldering [e], Xiong Liu [c], Vijay Natraj [e], Susan S. Kulawik [e]

[a] Department of Earth and Planetary Sciences, Harvard University, 29 Oxford Street, Cambridge, MA 02138, United States
[b] School of Engineering and Applied Sciences, Harvard University, Cambridge, MA, United States
[c] Harvard Smithsonian Center for Astrophysics, Cambridge, MA, United States
[d] Geophysical Fluid Dynamics Laboratory, NOAA, Princeton, NJ, United States
[e] Jet Propulsion Laboratory, California Institute of Technology, Pasadena, CA, United States

ARTICLE INFO

Article history:
Received 11 November 2010
Received in revised form
20 April 2011
Accepted 23 May 2011

Keywords:
Air quality
Ozone
Kalman filter
Assimilation
Remote sensing

ABSTRACT

We conduct an Observing System Simulation Experiment (OSSE) to test the ability of geostationary satellite measurements of ozone in different spectral regions to constrain surface ozone concentrations through data assimilation. Our purpose is to define instrument requirements for the NASA GEO-CAPE geostationary air quality mission over North America. We consider instruments using different spectral combinations of UV (290–340 nm), Vis (560–620 nm), and thermal IR (TIR, 9.6 μm). Hourly ozone data from the MOZART global 3-D chemical transport model (CTM) are taken as the "true" atmosphere to be sampled by the instruments for July 2001. The resulting synthetic data are assimilated in the GEOS-Chem CTM using a Kalman filter. The MOZART and GEOS-Chem CTMs have independent heritages and use different assimilated meteorological data sets for the same period, making for an objective OSSE. We show that hourly observations of ozone from geostationary orbit improve the assimilation considerably relative to daily observation from low earth orbit, and that broad observation over the ocean is unnecessary if the objective is to constrain surface ozone distribution over land. We also show that there is little propagation of ozone information from the free troposphere to the surface, so that instrument sensitivity in the boundary layer is essential. UV + Vis and UV + TIR spectral combinations improve greatly the information on surface ozone relative to UV alone. UV + TIR is preferable under high-sensitivity conditions with strong thermal contrast at the surface, but UV + Vis is preferable under low-sensitivity conditions. Assimilation of data from a UV + Vis + TIR instrument reduces the GEOS-Chem error for surface ozone by a factor of two. Observation in the TIR is critical to obtain ozone information in the upper troposphere relevant to climate forcing.

1. Introduction

Ozone in the troposphere is of importance as a surface air pollutant, as a greenhouse gas, and as the precursor of OH, the main atmospheric oxidant. It is produced by photochemical oxidation of carbon monoxide (CO) and volatile organic compounds (VOCs) in the presence of nitrogen oxide radicals ($NO_x \equiv NO + NO_2$). These precursors have both natural and anthropogenic sources. The dependence of ozone production on its precursors is complex and highly non-linear, and involves a continuum of time scales ranging from milliseconds to years. Our limited understanding of the factors controlling tropospheric ozone is reflected by the inability of current models to reproduce observed ozone trends over the past century (Mickley et al., 2001; Shindell and Faluvegi, 2002), including the past few decades (Fusco and Logan, 2003).

Over the past decade, observation of tropospheric ozone and its precursors from space has become an increasingly powerful tool for understanding the ozone budget (Martin, 2008). Current satellite instruments provide reliable measurements of ozone, CO, NO_2, and formaldehyde (HCHO) (Fishman et al., 2008). The Aura satellite includes direct measurements of tropospheric ozone by two instruments measuring in different spectral regions: the Tropospheric Emission Spectrometer (TES) in the thermal infrared (TIR) (Beer, 2006) and the Ozone Monitoring Instrument (OMI) in the UV (Levelt et al., 2006, Liu et al., 2010). Consistency between TES and OMI measurements has been demonstrated (Zhang et al., 2010). These data have been used to constrain models of tropospheric

* Corresponding author. Tel.: +1 617 496 5414; fax: +1 617 495 4551.
E-mail address: zoogman@fas.harvard.edu (P. Zoogman).
[1] Present address: Royal Netherlands Meteorological Institute, De Bilt, Netherlands.

1352-2310/$ – see front matter © 2011 Elsevier Ltd. All rights reserved.
doi:10.1016/j.atmosenv.2011.05.058

ozone, including the source from biomass burning (Bowman et al. 2008), intercontinental transport (Zhang et al., 2006), and greenhouse radiative forcing (Worden et al., 2008). Assimilation of TES ozone has been found to significantly improve modeled ozone concentrations in the free troposphere over North America (Parrington et al., 2008).

All satellite observations of tropospheric ozone and its precursors so far have been from sunsynchronous low earth orbit (LEO). They provide a global view but the return time over a given location is too long to track the low-altitude (boundary layer) variability relevant to ozone air quality (Fishman et al., 2008). An instrument in geostationary orbit could provide hourly data covering a continental scale (Campbell and Fishman, 2008), allowing monitoring of the progression of pollution events and the diurnal evolution of sources and chemistry. This would represent a transformative development for observing air quality from space. GEO-CAPE (Geostationary Coastal And Pollution Events), a NASA satellite mission planned for launch in the next decade, holds much promise in this regard (National Research Council (NRC), 2007). Parallel plans for geostationary missions directed at air quality are presently underway in Europe (Committee on Earth Observation Satellites, 2009) and in Korea (Lee et al., 2010).

Design of GEO-CAPE is at an early stage. The specific measurement requirements and observation strategy have not yet been determined. An Observing System Simulation Experiment (OSSE) framework is useful for this purpose. GEO-CAPE observations are intended to be assimilated into models to improve understanding of air quality and aid in its forecasting; an OSSE can address the question of how much information these observations will actually provide. In the OSSE framework, we generate synthetic ozone data from a chemical transport model (CTM) to represent the "true" atmosphere. We then examine the capability of different possible instrument configurations and observing strategies to deliver on the proposed scientific objectives through formal data assimilation into an independent CTM taken as forward model. OSSEs are the standard approach to quantify the potential benefit of a proposed observation platform toward a scientific goal (Lord et al., 1997). An OSSE study by Edwards et al. (2009) previously showed that geostationary CO observations would be significantly more effective than LEO observations in improving the ability of models to describe pollution events on a synoptic scale.

Here we present an OSSE for ozone air quality observations from geostationary orbit over North America, focusing on the potential capability of instruments measuring in different combinations of spectral ranges: UV + Visible (Vis), UV + TIR, and UV + Vis + TIR. We generate synthetic observations for July 2001 by having these different instruments "observe" 3-D ozone fields from the MOZART CTM (Fiore et al., 2011). These synthetic observations are then assimilated into the GEOS-Chem CTM (Park et al., 2006; Wang et al., 2009) and we quantify how much information each instrument configuration provides to reduce the difference between GEOS-Chem and the "true" MOZART atmosphere. The MOZART and GEOS-Chem CTMs have different heritages and use different assimilated meteorological fields for the same period, thus providing an OSSE with realistic error. Both are global CTMs, which is necessary because smoothing errors from satellite observations result in upper tropospheric information (transported on a global scale) influencing the lower tropospheric retrievals. They still have sufficient horizontal resolution to describe transport on synoptic scales, and sufficient vertical resolution to describe mass exchange between the free troposphere and the surface.

2. Ozone air quality measurements from GEO-CAPE

The NASA GEO-CAPE geostationary mission over North America was recommended by the 2007 NRC *Earth Science Decadal Survey* (NRC, 2007) as one of 14 top-priority satellite missions for NASA in the coming decade. GEO-CAPE has both an air quality and a coastal ecosystems component. Primary objectives of the air quality component include the mapping of emissions for ozone and aerosol precursors, the observation of ozone and aerosols with sensitivity near the surface, and the quantification of ozone and aerosol radiative forcing.

A major challenge for GEO-CAPE is the measurement of ozone with sensitivity near the surface. Direct satellite retrievals of tropospheric ozone have been made from solar backscattered UV spectra in the Hartley–Huggins bands (290–340 nm) (Liu et al., 2005, 2010) and from TIR emission in the 9.6 μm ν_3 band (Beer, 2006). These have poor sensitivity in the boundary layer, in the UV because of molecular scattering and in the TIR because of lack of thermal contrast. UV and TIR instruments have similar vertical sensitivities for tropospheric ozone as indicated by their averaging kernel matrices (Zhang et al., 2010). Theoretical studies have suggested that boundary layer sensitivity to ozone could be improved by using multispectral approaches involving UV + TIR (Worden et al., 2007; Landgraf and Hasekamp, 2007) or UV plus the weak Vis Chappuis band (560–620 nm) (Chance et al., 1997; Liu et al., 2005).

The retrieval sensitivity of vertical concentration profiles retrieved from satellite spectra can be expressed as an averaging kernel matrix **A** relating the retrieved profile $\mathbf{x}'$ to the true profile **x** and an *a priori* profile $\mathbf{x}_a$:

$$\mathbf{x}' = \mathbf{x}_a + \mathbf{A}(\mathbf{x} - \mathbf{x}_a) + \varepsilon \quad (1)$$

where ε is the random spectral measurement error (Rodgers, 2000). Averaging kernel matrices for tropospheric ozone profile retrievals in the different spectral combinations described above have been produced by the GEO-CAPE Simulation Team (Natraj et al., submitted for publication). We consider here clear-sky averaging kernel matrices from four spectral combinations: UV, UV + Vis, UV + TIR, and UV + Vis + TIR. The UV (290–340 nm) and Vis (560–620 nm) candidate sensors each have a spectral resolution of 0.4 nm and a signal to noise ratio three times that of OMI. The TIR (980–1070 cm^{-1}) sensor has a spectral resolution of 0.1 cm^{-1} and a signal to noise ratio three times that of TES. The averaging kernel matrices used in this analysis do not include the impacts of clouds and aerosols. Clouds and aerosols are expected to negatively impact Vis channels most strongly, as well as having some impact in the UV and TIR. Natraj et al. (submitted for publication) report multiple cases for each instrument, based on assumed atmospheric conditions. We select from their work a high-sensitivity case and a low-sensitivity case to characterize the range of instrument performance and provide upper and lower bounds on the information obtainable from geostationary observation. Sensitivity increases with higher thermal contrast between the surface and the atmosphere, higher boundary layer ozone concentration, higher surface albedo, and lower effective solar zenith angle.

Fig. 1 shows the rows of the averaging kernel matrices for the high-sensitivity and low-sensitivity cases weighted by level thickness. Also shown are the degrees of freedom for signal (DOFS) below given pressure levels. These are as given by Natraj et al. (submitted for publication). Each line (row) gives the vertical sensitivity of the ozone retrieval at a given level to the "true" profile. The DOFS are the number of independent pieces of information in the vertical provided by the retrieval, as determined from the trace of the averaging kernel matrix. Sensitivity of UV retrievals in the boundary layer is limited by air molecular scattering (0.27–0.54 DOFS below 800 hPa). When combined with UV, the Chappuis band adds information near the surface (0.64–0.77 DOFS below 800 hPa). In the Chappuis band there is reduced molecular scattering and ozone absorption is optically thin, resulting in better transmission and an increased signal from the boundary layer. Both

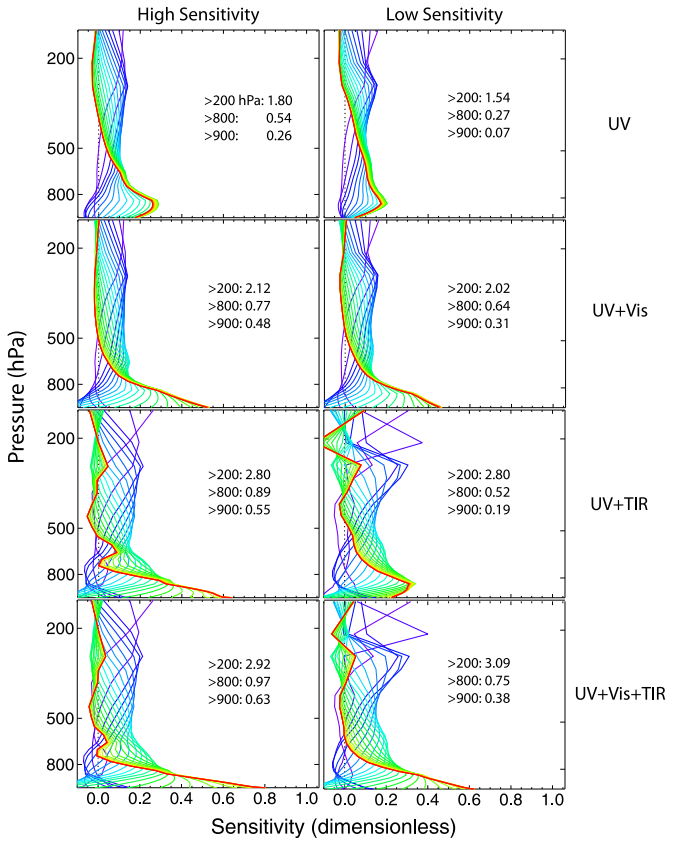

Fig. 1. Rows of typical averaging kernel matrices for theoretical retrievals of ozone vertical profiles from geostationary ozone instruments in different spectral combinations: UV, UV + Vis, UV + TIR, and UV + Vis + TIR (Natraj et al., submitted for publication). The color gradient from red to blue corresponds to retrievals at different levels from surface air (red) to 200 hPa (blue). Results from a high-sensitivity case (left) and a low-sensitivity case (right) are shown. Insets are the degrees of freedom for signal (DOFS) for the atmospheric columns below 200, 800, and 900 hPa. (For interpretation of the references to color in this figure legend, the reader is referred to the web version of this article.)

the UV and the UV + Vis retrievals provide more information in the high-sensitivity case than in the low-sensitivity case due to greater ozone concentrations in the boundary layer, higher surface albedo, and better viewing geometry. Retrievals in the TIR depend on the temperature contrast between the atmosphere and the surface as well as ozone concentration. Temperature contrast gives profile information in the upper troposphere, reflected in the peaks in the rows of the averaging kernels above 500 hPa for combinations including the TIR. In the high-sensitivity case there is a strong thermal contrast between the surface radiant (skin) temperature and the air temperature, resulting in increased boundary layer information from including the TIR (0.89 DOFS below 800 hPa). This enhancement is not as strong in the low-sensitivity case (0.52 DOFS below 800 hPa). For both cases the full UV + Vis + TIR combination provides the maximum information (0.75–0.95 DOFS below 800 hPa).

We used the adjoint of the GEOS-Chem ozone simulation (Henze et al., 2007; Zhang et al., 2009) to examine whether satellite information on ozone in the free troposphere would help constrain surface ozone through the forward propagation of information in the model by atmospheric transport. Fig. 2 illustrates the average sensitivity of surface ozone in eastern Massachusetts and southern California to ozone production at different altitudes for two weeks in July 2006. Most of the ozone in surface air is produced below 2 km altitude, although the sensitivity to the free troposphere is

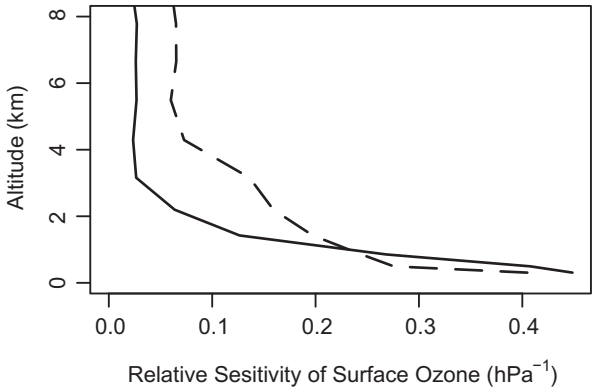

Fig. 2. Sensitivity of surface ozone over eastern Massachusetts (42°N, 72°W, solid) and southern California (34°N, 118°W, dashed) to integrated ozone production at different altitudes, as computed from the GEOS-Chem adjoint model for 1–14 July 2006.

stronger over southern California. We conclude that the GEO-CAPE instrument requires direct boundary layer sensitivity to constrain surface ozone. Our result is consistent with a CTM tracer study in support of the Infrared Atmospheric Sounding Interferometer (IASI) by Foret et al. (2009) which showed that on average only 7% of ozone at 800–700 hPa over Europe reaches the surface. Parrington et al. (2009) found that assimilation of TES free tropospheric ozone into GEOS-Chem affected the simulation of boundary layer ozone by 0–9 ppbv but did not systematically improve it.

3. OSSE framework

Our OSSE uses the MOZART CTM to represent the "true" atmosphere and the GEOS-Chem CTM as the forward model, both simulating the month of July 2001. Synthetic observations of the "true" atmosphere are made for different instrument configurations using the clear-sky averaging kernel matrices of Fig. 1. Comparing the model states without assimilation (*a priori*) and with assimilation (*a posteriori*) to the concentrations from the "true" atmosphere measures the information retrieved from the instrument configuration.

The GEOS-Chem simulation (v8-01-01) was previously described by Wang et al. (2009) in a study of Canadian and Mexican influences on US ozone air quality. It is driven by GEOS-3 assimilated meteorological data from the NASA Global Modeling and Assimilation Office (GMAO) with 6-h temporal resolution. It includes a full representation of tropospheric ozone–NO_x–VOC–aerosol chemistry over a nested North America domain with 1° × 1° horizontal resolution (10°N–60°N, 140°W–40°W), nested within a global domain with 4° × 5° horizontal resolution. It has 48 vertical levels, including 9 levels below 2 km and 17 levels below 10 km. It uses the Synoz flux boundary condition for the ozone source from the stratosphere (McLinden et al., 2000) For the purpose of the OSSE, ozone concentrations above the tropopause are replaced with MOZART values as described below.

For our "true" state we use hourly archived data from the MOZART-2 CTM (Fiore et al., 2011) driven by assimilated meteorological data from the National Center for Environmental Prediction (NCEP) with 1.8° × 1.8° horizontal resolution and 28 vertical levels (8 below 2 km, 17 below 10 km). This version of MOZART uses a modified version of the Synoz flux boundary condition for the ozone source from the stratosphere. The data are horizontally averaged on the 1° × 1° GEOS-Chem model grid. MOZART has a separate development heritage from GEOS-Chem and uses different driving meteorological fields, chemical mechanisms, and emission inventories. There is little commonality in any aspect of the tropospheric models, which is an important attribute for our

OSSE study. The coarse horizontal resolution of MOZART means that our OSSE cannot test the ability of GEO-CAPE to constrain urban-scale features and mesoscale transport of ozone. However, our focus here is on vertical sensitivity.

Fig. 3 shows the maximum daily 8-h average (MDA8) ozone concentrations in the lower free troposphere (700 hPa) and in surface air for each model for July 2001. GEOS-Chem is higher than MOZART in the free troposphere over most of the domain. At the surface the patterns tends to reverse, with MOZART higher than GEOS-Chem over much of the US Northeast and Midwest. Thus the vertical gradients of ozone differ greatly between the two models, presenting the OSSE with a challenging test. Gradient reversals between the free troposphere and the surface are consistent with our results in Fig. 2 showing boundary layer ozone to be primarily constrained by production below 2 km.

We generate synthetic geostationary observations from the MOZART "true" atmosphere by sampling the hourly daytime vertical profiles over the whole domain with the averaging kernel matrices given in Fig. 1. We do not sample at night, as UV + Vis observations are not available and TIR observations have less information than in daytime. We also omit scenes with cloud fraction >0.3 (as given by the GEOS-3 meteorology). Gaussian random error is added to the synthetic observations to simulate spectral measurement error (instrument noise ε in eq. (1)) as given by Natraj et al. (submitted for publication). As the GEO-CAPE footprint (~8 km) is much finer than the GEOS-Chem resolution (~100 km), the instrument error is reduced by the square root of the number of observations available for the corresponding GEOS-Chem grid square. In the OSSE framework we assimilate the synthetic observations of the "true" state into the forward model, as we would do with actual data, to correct the mismatch between the "true" and *a priori* states. We do this sequentially by using a Kalman filter following Khattatov et al. (2000). A Kalman filter provides the best estimate of the state at a given time step using measurements at that time step and *a priori* information from previous time steps of the model (Rodgers, 2000). We apply the filter iteratively at successive observation time steps to update the model state.

At an observation time step t we combine the local synthetic observed ozone profile $\mathbf{x}'_t$ (from eq. (1)) with the model ozone profile $\mathbf{x}_{at}$ to find the *a posteriori* ozone concentration $\hat{\mathbf{x}}_t$:

$$\hat{\mathbf{x}}_t = \mathbf{x}_{at} + \mathbf{G}_t(\mathbf{x}'_t - \mathbf{K}_t\mathbf{x}_{at}) \tag{2}$$

where $\mathbf{K}_t$ is the observation operator at time step t which maps the true state to the observed state. This represents the measurement process and in our case is the instrument averaging kernel matrix, assumed to be invariant ($\mathbf{K}_t = \mathbf{A}$). $\mathbf{G}_t$ is the Kalman gain matrix given by:

$$\mathbf{G}_t = \mathbf{S}_{at}\mathbf{K}^T\left(\mathbf{K}\mathbf{S}_{at}\mathbf{K}^T + \mathbf{S}_\varepsilon\right)^{-1} \tag{3}$$

The gain matrix determines the relative weight given to the observations and the model. It depends on the error covariance matrices for the observations $\mathbf{S}_\varepsilon = [\varepsilon\varepsilon^T]$ and for the model $\mathbf{S}_{at}$. Above the tropopause we replace the GEOS-Chem simulated profiles with the synthetic retrievals so that the innovation term $\mathbf{x}'_t - \mathbf{K}_t\mathbf{x}_{at}$ is solely determined by the tropospheric simulation. We used this method in the past to avoid having stratospheric errors in GEOS-Chem affect model comparisons with satellite data for tropospheric ozone (Zhang et al., 2006).

The model error $\mathbf{S}_{a0}$ is initialized using the Relative Residual Error (RRE) method (Palmer et al., 2003; Heald et al., 2004) by comparing GEOS-Chem ozone profiles to colocated ozonesonde measurements for 2006 (Zhang et al., 2010). We find that the RRE of GEOS-Chem ozone is 25% on an annual global basis and 29% for North America in summer, with no significant vertical dependence. We use 29% to specify the initial model error variances. The spatial model error covariance is parameterized by an exponential length scale as in Khattatov et al. (2000), with a length scale of 1 km in the vertical and 100 km in the horizontal.

The model error covariance is reduced by the data assimilation at each observation time step:

$$\widehat{\mathbf{S}}_t = (\mathbf{I} - \mathbf{G}_t\mathbf{K}_t)\mathbf{S}_{at} \tag{4}$$

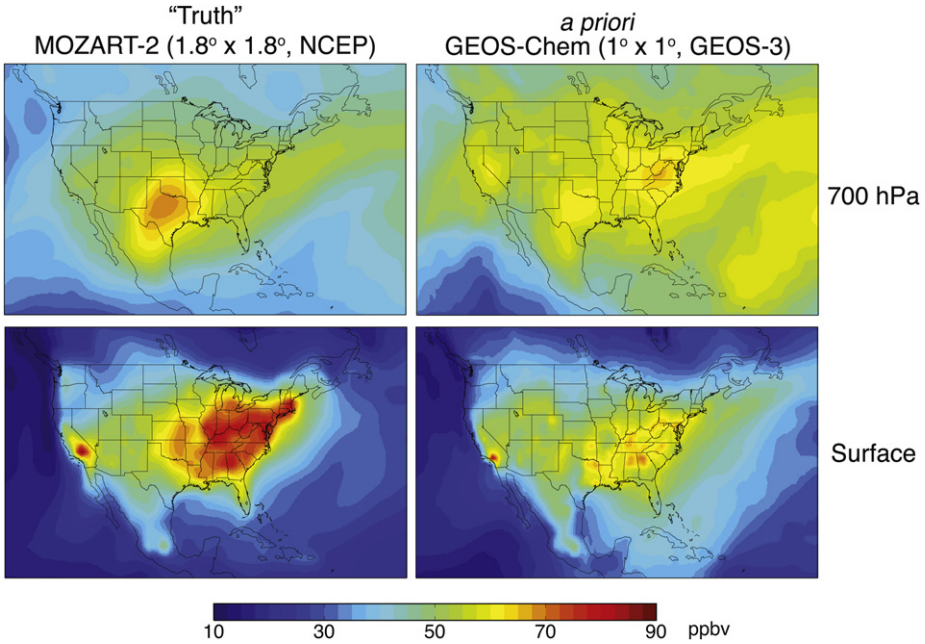

Fig. 3. Mean 8-h daily maximum ozone concentrations for July 2001 at 700 hPa and in surface air. Left panels show values from the MOZART CTM used as the "true" atmosphere in our OSSE. Right panels show the *a priori* values from the GEOS-Chem CTM.

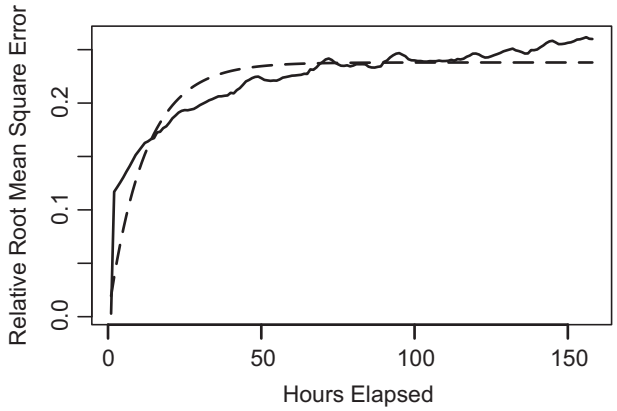

Fig. 4. Temporal evolution of the ozone concentration error in GEOS-Chem relative to MOZART, as determined by comparing GEOS-Chem and MOZART fields in simulations with a common initialization at 0 GMT on July 1 2001. The error statistics are measured by the relative root-mean-square error (RRMSE) for the concentration fields sampled over the North America domain. Results (solid) are fitted to an exponential function (dashed) for application to model error growth in our Kalman filter. The exponential fit gives an asymptotic error of 24% approached on a time scale of 12 h.

where $\widehat{\mathbf{S}}_t$ is the updated model error covariance matrix. The diagonal terms of $\widehat{\mathbf{S}}_t$ are transported as tracers in GEOS-Chem to the next time step and are augmented by a model error variance reflecting the time-dependent divergence of the model from the true state. We quantified this time-dependent error growth in a separate test comparing MOZART and GEOS-Chem evolution of ozone concentrations, starting from identical initial tropospheric ozone fields at 0 GMT on 1 July, 2001. Results in Fig. 4 show an exponential relaxation of the model relative root-mean-square error (RRMSE) with time for the simulation of ozone concentrations in the ensemble of tropospheric model grid-boxes over North America. The asymptotic RRMSE (24%) is approached on a time scale of 12 h following initialization. The agreement between this asymptotic value and the GEOS-Chem RRE in comparison to ozonesonde data indicates that differences between GEOS-Chem and MOZART are consistent with expected model errors relative to observations. This is an important check on the quality of the OSSE.

We checked the good behavior of our Kalman filter by comparing the mean and variance of our calculated innovation terms $\mathbf{x}'_t - \mathbf{K}_t\mathbf{x}_{at}$ to theoretical statistical predictions following Rodgers (2000). Theoretically, the innovation should be a normally distributed random variable with a mean equal to the model bias (here GEOS-Chem vs. MOZART) and a covariance equal to $\mathbf{K}\mathbf{S}_{at}\mathbf{K}^T + \mathbf{S}_\varepsilon$. We find that this is indeed the case.

4. Performance of different instrument configurations

Here we examine the ability of different instrument configurations and observing modes to constrain surface ozone over the US domain (25°N–50°N, 125°W–65°W, land only). We use as our comparison metric the Root-Mean-Square Error (RMSE) of MDA8 ozone. The RMSE is computed only over the US, but observations are assimilated over the entire North America nested domain (10°N–60°N, 140°W–40°W) unless otherwise specified.

We first examine the value of making observations from geostationary vs. LEO. This is done using two simulations. In the first, we assimilate observations once daily at 1300 local time (LEO). In the second, we assimilate observations once per hour during the daytime (geostationary orbit). Both simulations use the same averaging kernel matrix from the high-sensitivity case for the UV + Vis + TIR instrument (Fig. 1). Both are initialized on July 1 with the *a priori* GEOS-Chem ozone fields. Fig. 5 shows the *a priori* bias and *a posteriori* bias in MDA8 ozone averaged over July 2001 for each 1° × 1° grid

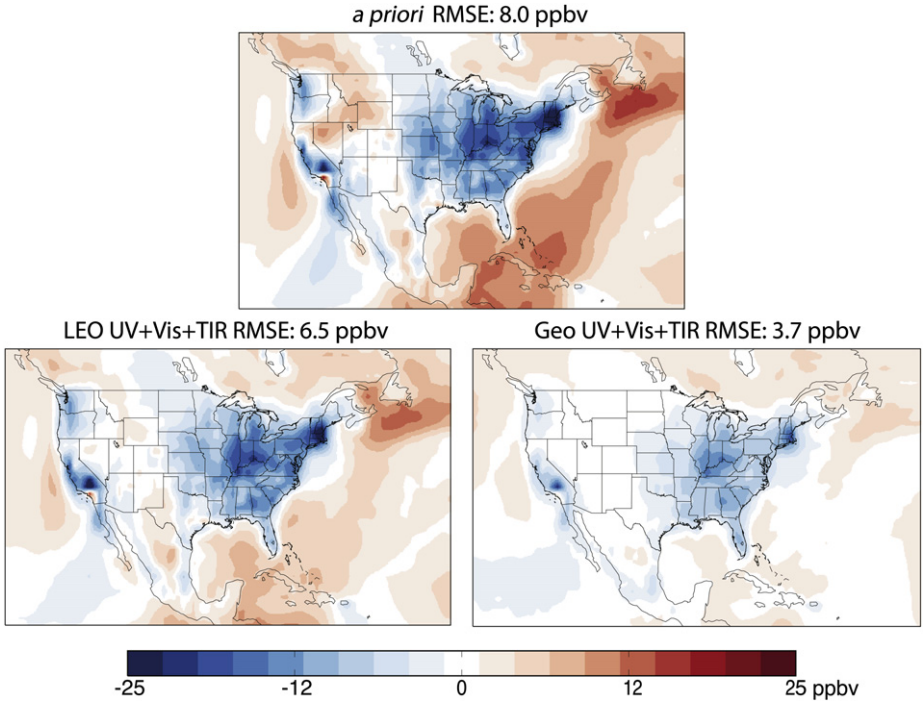

Fig. 5. Mean bias for July 2001 in MDA8 surface ozone concentrations between the GEOS-Chem model and the MOZART model taken as the "true" atmosphere. The top panel shows the *a priori* bias before assimilation. The bottom panels show the model biases after assimilation of synthetic observations from the "true" atmosphere on a daily basis simulating a LEO instrument (left) and on an hourly basis simulating a geostationary instrument (right). The synthetic observations are for daytime only and assume a UV + Vis + TIR instrument under high-sensitivity conditions (Fig. 1). Error statistics for the contiguous US are given as the root-mean-square error (RMSE).

square. The *a priori* RMSE is 8.0 ppbv ozone. The hourly observations reduce the RMSE by 54% as compared to a 19% reduction by the daily observations. We see that the hourly observations enabled by geostationary orbit allow the model to much better capture the magnitude and spatial distribution of surface ozone.

One question in GEO-CAPE design is whether observing over the ocean would improve information on US air quality. In a separate simulation, we assimilate hourly UV + Vis + TIR ozone observations as above, except with observations only over land scenes. We find that removing ocean scenes from the observing domain does not significantly impact the general ability to constrain surface ozone over the US domain (2% increase of ozone RMSE). Although there is clearly a need to extend geostationary observations some distance offshore to improve information for coastal areas (an issue that we cannot investigate at the horizontal resolution of our OSSE), we do not find a broader benefit of ocean observations for constraining US ozone air quality. Synoptic-scale recirculation of continental air masses transported offshore has occasionally been found to contribute to regional pollution episodes in the eastern US, but once these air masses are advected back over land domain they would be observed and assimilated into the model.

We now investigate the effectiveness of various spectral combinations. We simulate daytime hourly observations in the UV, UV + Vis, UV + TIR, and UV + Vis + TIR, for both the high-sensitivity and low-sensitivity cases. These two cases can be viewed as representing upper and lower bounds respectively for the information achievable from the observations. The spatial pattern of the correction is similar in each case to that in Fig. 5, so that we use the RMSE as a single comparison statistic as described above. Fig. 6 shows the RMSE of MDA8 ozone over the US for all of the spectral combinations and cases simulated. In the low-sensitivity case, the UV only observations (with an improved OMI-like instrument) provide a small correction, reducing the RMSE by 12% relative to the *a priori*. The full UV + Vis + TIR observations, on the other hand, remove half the *a priori* RMSE. In this low-sensitivity case, adding the TIR to the UV provides less corrective power (34% reduction in RMSE) than adding the Vis (41% reduction). The relative benefit of the different combinations is different in the high-sensitivity case, where thermal contrast is stronger. While the effectiveness of the UV + Vis instrument changes little, the TIR adds much more information near the surface than it did in the low-sensitivity case, reducing the RMSE by an additional 17%. In this scenario, the UV + TIR instrument is almost as successful as the UV + Vis + TIR instrument in correcting the *a priori* error.

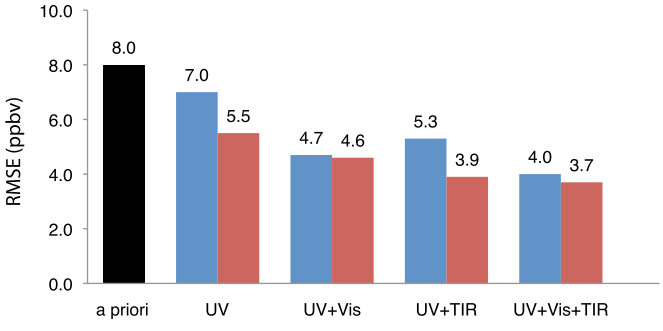

Fig. 6. Ability of geostationary ozone measurements in different spectral combinations to constrain the ozone surface air concentration over the US. The figure shows the root-mean-square error (RMSE) of 8-h maximum daily average (MDA8) ozone over the continental US in July 2001 relative to the "true" state defined by the MOZART model. The *a priori* error from the GEOS-Chem simulation is compared to the *a posteriori* errors after assimilation of observations from instruments in the different spectral combinations, for the high-sensitivity (red) and low-sensitivity (blue) cases of Fig. 1. (For interpretation of the references to color in this figure legend, the reader is referred to the web version of this article.)

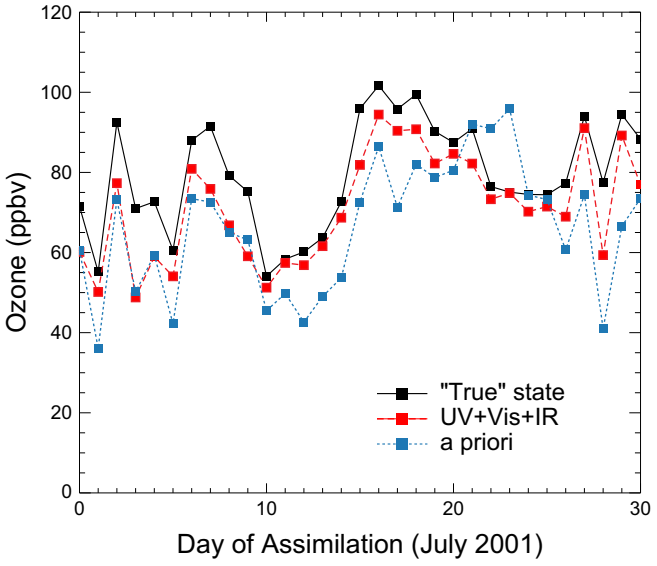

Fig. 7. Time series of MDA8 surface ozone at Pittsburgh (40°N, 80°W) in July 2001 for the "true" state, the model *a priori*, and the model *a posteriori* with assimilated UV1bservations.

A goal for the GEO-CAPE mission is to improve air quality mapping and forecasts on daily time scales. Fig. 7 shows a typical July time series of MDA8 surface ozone at Pittsburgh for the "true" state, the model *a priori*, and the model *a posteriori* with assimilated UV + Vis + IR observations from the high-sensitivity case. The assimilation greatly improves the ability of the model to reproduce the daily variability in MDA8 surface ozone (*a posteriori* $R^2 = 0.84$ vs. *a priori* $R^2 = 0.52$). Of particular interest is the ability of the assimilation to capture ozone exceedances of the current US air quality standard of 75 ppbv. During July, the "true" state for Pittsburgh experiences 19 days with MDA8 ozone greater than 75 ppbv.

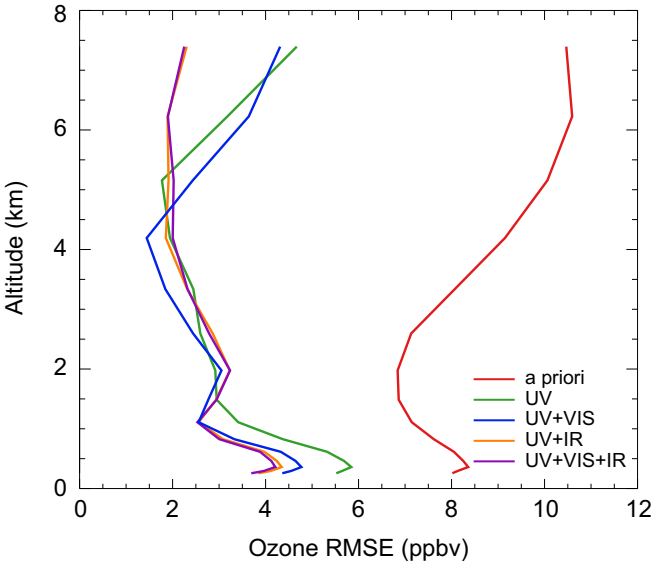

Fig. 8. Ability of geostationary ozone measurements in different spectral combinations to constrain the vertical profile of tropospheric ozone. The figure shows the root-mean-square error (RMSE) of ozone concentrations over the continental US vs. altitude in July 2001 relative to the "true" atmosphere defined by the MOZART model. The *a priori* error from the GEOS-Chem simulation is compared to the *a posteriori* errors after assimilation of observations from instruments in the different spectral combinations. Results are for the high-sensitivity case of Fig. 1.

In comparison, the model *a priori* model only has 7 exceedances, while the model *a posteriori* has 13 exceedances. There are no false positives. Over the US the "true" state experiences 4250 MDA8 ozone exceedances during July. The model *a priori* has 3513 false negatives and 288 false positives, while the model *a posteriori* has 2221 false negatives (37% fewer) and 49 false positives (83% fewer).

Better quantifying ozone climate forcing and its relationship to sources is also a GEO-CAPE objective. This requires sensitivity to the middle and upper troposphere where ozone climate forcing is most efficient. Fig. 8 shows the vertical profiles of the ozone RMSE for each spectral combination, averaged over the US domain. The influence of stratospheric air is minimized by design of the OSSE (Section 3). Results are shown for the high-sensitivity case: the vertical information content is similar in the low-sensitivity case except near the surface (Fig. 1). Observing in the UV alone reduces model error most efficiently in the middle troposphere between 2 and 5 km, least efficiently in the upper troposphere and near the surface. Adding Vis coverage significantly reduces the error near the surface but not at higher altitudes. Adding TIR coverage reduces the error both near the surface and in the upper troposphere, though it has little effect between 2 and 5 km. UV + Vis + TIR does not add significant information relative to UV + TIR, though we have seen previously that Vis is effective in reducing error at the surface for the low-sensitivity case.

5. Summary

We conducted an observing system simulation experiment (OSSE) to determine the instrument requirements for geostationary satellite observations of ozone air quality in the US. Our aim was to inform the design of the NASA GEO-CAPE mission planned for launch by NASA in the 2020 time frame. We considered combinations of UV (Hartley–Huggins bands), Vis (Chappuis band), and TIR (9.6 μm ν_3 band) spectral regions for the candidate ozone instruments. While UV and TIR retrievals have been used before for ozone measurements from LEO, they lack sensitivity in the boundary layer which is important for air quality. The Chappuis band can provide this sensitivity. A sensitivity simulation with the adjoint of the GEOS-Chem model shows that most of the ozone in polluted areas of the US in summer is produced within the boundary layer, emphasizing the importance of sensitivity in that region.

Our OSSE framework uses 3-D hourly archives of ozone concentrations from the MOZART chemical transport model (CTM) for July 2001 as a "true" atmosphere to be sampled by the candidate instruments. We assimilate these pseudo-observations into the GEOS-Chem CTM for that month using a Kalman filter. The MOZART and GEOS-Chem CTMs have very different heritages and use different assimilated meteorological data sets, making for an objective OSSE. The error statistics between GEOS-Chem and MOZART are similar to those between GEOS-Chem and ozonesonde observations, further confirming the quality of this OSSE framework.

Our OSSE results indicate that hourly daytime observations of ozone achievable from geostationary orbit provide much better constraints on surface ozone than LEO daily observations. We also find that the geostationary observing domain can be limited to the North American continent if the measurement objective is to constrain US ozone air quality, as observations over adjacent oceans provide little additional information. We find that multispectral observations provide much more information for surface ozone air quality than UV only. A UV + TIR combination is successful for high-sensitivity conditions with strong thermal contrast at the surface, but a UV + Vis combination performs better under low-sensitivity conditions. A UV + Vis + TIR combination corrects half of the *a priori* error in surface ozone. Observation in the TIR is critical to obtain ozone information in the upper troposphere relevant to climate forcing.

As part of calculating error covariance matrices for ozone data assimilation, we examined the time-dependent growth of the difference in surface air ozone concentrations simulated by GEOS-Chem and MOZART following common initialization. We find that the root-mean-square error (RMSE) between the two models reaches its asymptotic value (24%) on a time scale of only 12 h. This means that ozone data assimilation in our OSSE environment would not enable useful air quality forecasts.

Our OSSE framework provides a general facility for addressing measurement requirements for GEO-CAPE. A limitation of the present study is the use of invariant averaging kernel matrices for the different instrument configurations. Our high-sensitivity and low-sensitivity cases can be viewed as providing upper and lower bounds for the information achievable from geostationary observation. We will improve in future work by using variable averaging kernel matrices responding to changes in environmental conditions. Shortcomings from using a coarse-scale "truth" model will be addressed in future work by using a regional CTM as the "truth" state. We will also examine the usefulness of complementary satellite measurements of other species (CO, NO_2, HCHO) for constraining surface ozone.

Acknowledgments

This work was supported by the NASA Atmospheric Composition and Modeling Program, by the NASA Earth Science Division, Flight Directorate, and by a NASA Earth and Space Science Fellowship to Peter Zoogman.

References

Beer, R., 2006. TES on the aura mission: scientific objectives, measurements, and analysis overview. IEEE Transactions on Geoscience and Remote Sensing 44, 1102–1105.

Bowman, K.W., Jones, D.B.A., Logan, J.A., Worden, H., Boersma, F., Kulawik, S., Chang, R., Osterman, G., Worden, J., 2008. The zonal structure of tropical O3 and CO as observed by the Tropospheric Emission Spectrometer in November 2004. Part II. Impact of surface emissions on O3 and its precursors. Atmospheric Chemistry and Physics.

Campbell, J., Fishman, J., 2008. NASA GEO-CAPE Workshop Report. http://geo-cape.larc.nasa.gov/docs/GEO-CAPE_Wkshp_RPt_Final-all.pdf.

Chance, K.V., Burrows, J.P., Perner, D., Schneider, W., 1997. Satellite measurements of atmospheric ozone profiles, including tropospheric ozone, from ultraviolet/visible measurements in the nadir geometry: a potential method to retrieve tropospheric ozone. Journal of Quantitative Spectroscopy & Radiative Transfer 57, 467–476.

Committee on Earth Observation Satellites, 2009. Report on the Committee on Earth Observation Satellites Atmopsheric Composition Constellation Workshop on Air Quality. http://ceos.org/images/ACC-4Reportfinal.pdf.

Edwards, D.P., Arellano, A.F., Deeter, M.N., 2009. A satellite observation system simulation experiment for carbon monoxide in the lowermost troposphere. Journal of Geophysical Research-Atmospheres 114.

Fiore, A.M., Levy, H., Jaffe, D.A., 2011. North American isoprene influence on intercontinental ozone pollution. Atmospheric Chemistry and Physics 11, 1697–1710.

Fishman, J., Bowman, K.W., Burrows, J.P., Richter, A., Chance, K.V., Edwards, D.P., Martin, R.V., Morris, G.A., Pierce, R.B., Ziemke, J.R., Al-Saadi, J.A., Creilson, J.K., Schaack, T.K., Thompson, A.M., 2008. Remote sensing of tropospheric pollution from space. Bulletin of the American Meteorological Society 89, 805–821.

Foret, G., Hamaoui, L., Schmechtig, C., Eremenko, M., Keim, C., Dufour, G., Boynard, A., Coman, A., Ung, A., Beekmann, M., 2009. Evaluating the potential of IASI ozone observations to constrain simulated surface ozone concentrations. Atmospheric Chemistry and Physics 9, 8479–8491.

Fusco, A.C., Logan, J.A., 2003. Analysis of 1970–1995 trends in tropospheric ozone at Northern Hemisphere midlatitudes with the GEOS-CHEM model. Journal of Geophysical Research-Atmospheres 108.

Heald, C.L., Jacob, D.J., Jones, D.B.A., Palmer, P.I., Logan, J.A., Streets, D.G., Sachse, G.W., Gille, J.C., Hoffman, R.N., Nehrkorn, T., 2004. Comparative inverse analysis of satellite (MOPITT) and aircraft (TRACE-P) observations to estimate Asian sources of carbon monoxide. Journal of Geophysical Research-Atmospheres 109.

Henze, D.K., Hakami, A., Seinfeld, J.H., 2007. Development of the adjoint of GEOS-Chem. Atmospheric Chemistry and Physics 7, 2413–2433.

Khattatov, B.V., Lamarque, J.F., Lyjak, L.V., Menard, R., Levelt, P., Tie, X.X., Brasseur, G.P., Gille, J.C., 2000. Assimilation of satellite observations of long-lived chemical species in global chemistry transport models. Journal of Geophysical Research-Atmospheres 105, 29135–29144.

Landgraf, J., Hasekamp, O.P., 2007. Retrieval of tropospheric ozone: the synergistic use of thermal infrared emission and ultraviolet reflectivity measurements from space. Journal of Geophysical Research-Atmospheres 112.

Lee, T.F., Nelson, C.S., Dills, P., Riishojgaard, L.P., Jones, A., Li, L., Miller, S., Flynn, L.E., Jedlovec, G., McCarty, W., Hoffman, C., McWilliams, G., 2010. NPOESS next-generation operational global earth observations. Bulletin of the American Meteorological Society 91, 727.

Levelt, P.F., Van den Oord, G.H.J., Dobber, M.R., Malkki, A., Visser, H., de Vries, J., Stammes, P., Lundell, J.O.V., Saari, H., 2006. The ozone monitoring instrument. IEEE Transactions on Geoscience and Remote Sensing 44, 1093–1101.

Liu, X., Sioris, C.E., Chance, K., Kurosu, T.P., Newchurch, M.J., Martin, R.V., Palmer, P.I., 2005. Mapping tropospheric ozone profiles from an airborne ultraviolet–visible spectrometer. Applied Optics 44, 3312–3319.

Liu, X., Bhartia, P.K., Chance, K., Spurr, R.J.D., Kurosu, T.P., 2010. Ozone profile retrievals from the ozone monitoring instrument. Atmospheric Chemistry and Physics 10, 2521–2537.

Lord, S.J., Kalnay, E., Daley, R., Emmitt, G.D., Atlas, R., 1997. Using OSSEs in the Design of Future Generation Integrated Observing Systems. Preprints, 1st Symposium on Integrated Observing Systems. AMS, Long Beach, CA, 45–47 pp.

Martin, R.V., 2008. Satellite remote sensing of surface air quality. Atmospheric Environment 42, 7823–7843.

McLinden, C.A., Olsen, S.C., Hannegan, B., Wild, O., Prather, M.J., Sundet, J., 2000. Stratospheric ozone in 3-D models. Journal of Geophysical Research 105, 14653–14665.

Mickley, L.J., Jacob, D.J., Rind, D., 2001. Uncertainty in preindustrial abundance of tropospheric ozone: implications for radiative forcing calculations. Journal of Geophysical Research-Atmospheres 106, 3389–3399.

Natraj, V., Liu, X., Kulawik, S.S., Chance, K., Chatfield, R., Francis, G., Edwards, D., Eldering, A., Kurosu, T.P., Pickering, K., Spurr, R.J.D., Worden, H.M. Pan-spectral sensitivity studies for the retrieval of tropospheric and boundary layer ozone from simulated GEO-CAPE measurements. Atmospheric Environment, submitted for publication.

National Research Council, 2007. Earth Science and Applications from Space: National Imperatives for the Next Decade and Beyond. National Academy Press, Washington, D.C.

Palmer, P.I., Jacob, D.J., Fiore, A.M., Martin, R.V., Chance, K., Kurosu, T.P., 2003. Mapping isoprene emissions over North America using formaldehyde column observations from space. Journal of Geophysical Research-Atmospheres 108, 4804.

Park, R.J., Jacob, D.J., Kumar, N., Yantosca, R.M., 2006. Regional visibility statistics in the United States: natural and transboundary pollution influences, and implications for the regional Haze rule. Atmospheric Environment 40, 5405–5423.

Parrington, M., Jones, D.B.A., Bowman, K.W., Horowitz, L.W., Thompson, A.M., Tarasick, D.W., Witte, J.C., 2008. Estimating the summertime tropospheric ozone distribution over North America through assimilation of observations from the tropospheric emission spectrometer. Journal of Geophysical Research-Atmospheres 113.

Parrington, M., Jones, D.B.A., Bowman, K.W., Thompson, A.M., Tarasick, D.W., Merrill, J., Oltmans, S.J., Leblanc, T., Witte, J.C., Millet, D.B., 2009. Impact of the assimilation of ozone from the tropospheric emission spectrometer on surface ozone across North America. Geophysical Research Letters 36.

Rodgers, C.D., 2000. Inverse Methods for Atmospheric Sounding. World Scientific, River Edge, New Jersey.

Shindell, D.T., Faluvegi, G., 2002. An exploration of ozone changes and their radiative forcing prior to the chlorofluorocarbon era. Atmospheric Chemistry and Physics 2, 363–374.

Wang, H.Q., Jacob, D.J., Le Sager, P., Streets, D.G., Park, R.J., Gilliland, A.B., van Donkelaar, A., 2009. Surface ozone background in the United States: Canadian and Mexican pollution influences. Atmospheric Environment 43, 1310–1319.

Worden, J., Liu, X., Bowman, K., Chance, K., Beer, R., Eldering, A., Gunson, M., Worden, H., 2007. Improved tropospheric ozone profile retrievals using OMI and TES radiances. Geophysical Research Letters 34.

Worden, H.M., Bowman, K.W., Worden, J.R., Eldering, A., Beer, R., 2008. Satellite measurements of the clear-sky greenhouse effect from tropospheric ozone. Nature Geoscience 1, 305–308.

Zhang, L., Jacob, D.J., Bowman, K.W., Logan, J.A., Turquety, S., Hudman, R.C., Li, Q.B., Beer, R., Worden, H.M., Worden, J.R., Rinsland, C.P., Kulawik, S.S., Lampel, M.C., Shephard, M.W., Fisher, B.M., Eldering, A., Avery, M.A., 2006. Ozone-CO correlations determined by the TES satellite instrument in continental outflow regions. Geophysical Research Letters 33.

Zhang, L., Jacob, D.J., Kopacz, M., Henze, D.K., Singh, K., Jaffe, D.A., 2009. Intercontinental source attribution of ozone pollution at western US sites using an adjoint method. Geophysical Research Letters 36.

Zhang, L., Jacob, D.J., Liu, X., Logan, J.A., Chance, K., Eldering, A., Bojkov, B.R., 2010. Intercomparison methods for satellite measurements of atmospheric composition: application to tropospheric ozone from TES and OMI. Atmospheric Chemistry and Physics 10, 4725–4739.